Nanoporous GaN by selective area sublimation through an epitaxial nanomask: AlN versus Si_xN_y

B Damilano, S. Vézian, J. Brault, P Ruterana, B. Gil, M. Tchernycheva

Nanoporous GaN by selective area sublimation through an epitaxial nanomask: AlN vs Si_xN_y

B. Damilano,[1,a)] S. Vézian,[1] J. Brault,[1] P. Ruterana,[2] B. Gil,[3] M. Tchernycheva[4]

[1]Université Côte d'Azur, CNRS, CRHEA, Rue B. Gregory, Valbonne

[2]Centre de Recherche sur les Ions, les Matériaux et la Photonique, CIMAP-ENSICAEN, UMR 6252, 6 Boulevard Maréchal Juin 14050, Caen

[3]Laboratoire Charles Coulomb, UMR 5221 CNRS-Université de Montpellier, F-34095 Montpellier, France

[4]Centre de Nanosciences et de Nanotechnologies (C2N), UMR 9001 CNRS, Université Paris-Saclay, 10 Boulevard Thomas Gobert, Palaiseau 91120, France

[a)]Author to whom correspondence should be addressed : bd@crhea.cnrs.fr

Abstract

Nanoporous GaN layers were fabricated using selective area sublimation through a self-organized AlN nanomask in a molecular beam epitaxy reactor. The obtained pore morphology, density and size were measured using plan-view and cross-section scanning electron microscopy experiments. It was found that the porosity of the GaN layers could be adjusted from 0.04 to 0.9 by changing the AlN nanomask thickness and sublimation conditions. The room temperature photoluminescence properties as a function of the porosity were analysed. In particular, a strong improvement (>100) of the room temperature photoluminescence intensity was observed for porous GaN layers with a porosity in the 0.4-0.65 range. The characteristics of these porous layers were compared to those obtained with a Si_xN_y nanomask. Furthermore, the regrowth of p-type GaN on light emitting diode structures made porous by using either an AlN or a Si_xN_y nanomask were compared.

1. Introduction

Making porous a semi-conductor offers an additional degree of freedom to tune its physical properties. This is an attractive way to modify, for example, the optical properties, the thermal and electrical conductivity, the strain state of the crystal, etc...[1][2][3][4][5] Also, thanks to the high surface to volume ratio, porous semi-conductors can constitute highly reactive and sensitive materials.[6] In the case of group III-nitride semi-conductors, devices including porous material or porous devices were demonstrated.[7][8][9][10][11][12][13][14] The most common technique to make porous GaN is based on electrochemical etching.[15] Alternative techniques to make porous GaN with specific properties are also possible,[16] in particular we have previously shown that nanoporous GaN layers can be obtained with a top-down approach using selective area sublimation through a Si_xN_y uncomplete mono-layer.[17][18] The room temperature photoluminescence intensity of porous thin GaN layers on silicon substrate made by this method is increased by several orders of magnitude and the radiative lifetime is considerably shortened compared to non-porous layers.[19] The huge enhancement of the optical properties was mainly attributed to the preferential sublimation of the non-radiative dislocation cores as shown by transmission electron microscopy studies.[20] As the sublimation process is not dependent on the doping, fully porous InGaN/GaN light emitting diodes can be demonstrated by this technique.[21] Up to now, only Si_xN_y was used as a nanomask and it is not known whether other compounds can replace Si_xN_y and can lead to the formation of nanoporous GaN. Also, Si_xN_y has an anti-surfactant effect on the growth of GaN [22] and this has an influence on layer overgrowth onto porous structures.

In this work, we explore the use of AlN as a nanomask to make porous GaN by sublimation. We will compare the results to those obtained with a Si_xN_y nanomask in previous works. Finally, we will determine the impact of the nanomask material used during the regrowth on nanoporous LED structures.

2. Nanoporous GaN by selective area sublimation through an AlN Nanomask

a. Description of the samples

The samples were grown by molecular beam epitaxy on 2 inch Si(111) substrates using ammonia as the nitrogen precursor and solid sources for Al and Ga. For all the samples, the epitaxial growth is started by an AlN buffer layer (100-120 nm) and followed by a GaN layer (240-280 nm). The growth temperature is 900°C for the AlN buffer and 800°C for GaN. The dislocation density was estimated on a similar sample to be larger than $7x10^{10}$ cm^{-2}. Three reference non-porous (NP) samples were made.

NP1 is the simple AlN/GaN stack. Additional 2.5 mono-layers (MLs) of AlN are grown on top of GaN for NP2. NP3 has the same structure than NP2, but an annealing up to 900°C is performed with an ammonia flow of 10 standard centimeter cube per minute (sccm) during 4 min. This corresponds to the temperature ramp conditions used for all the porous samples (P). This sample was made in order to investigate whether the temperature ramp at high temperature could have an impact on the optical properties.

Four samples (P1, P2, P3, P4) were made porous. The initial layer stack is the same than for the NP samples. An AlN layer with a thickness ranging between 1 and 5 MLs is grown on top of the GaN (see Table 1). Then, the samples are heated up to 900°C using the same ramp than for NP3 sample. The ammonia flow is then decreased to an effective flow of ~2 sccm using pulsed conditions (one cycle corresponds to 1s under ammonia with a flow of 10 sccm and 4s without ammonia), for a duration indicated in Table 1. This provokes the selective area sublimation of GaN and the formation of pores. Note that under these conditions, the sublimation rate is decreased by a factor of 2 compared to sublimation under vacuum.

Table 1. Some characteristics of the samples used for the study of the porosification using an AlN nanomask. The AlN nanomask thickness range refers to the values corresponding at the center to the edge of the wafers. The asterix indicates that for this sample, after the AlN nanomask growth, the wafer temperature is ramped to 900°C in 4 min before the final cooling.

Sample	AlN nanomask thickness (ML)	Sublimation time (min)	Pore depth (nm)	Pores down to AlN buffer layer?
NP1	-	-	-	-
NP2	2.5-1.8	-	-	-
NP3	2.5-1.8	-*	-	-
NP4	-	-	-	-
P1	4.7-3.3	25	280	Yes
P2	3.1-2.2	30	268	Yes
P3	2.5-1.8	20	191	No
P4	1.1-0.7	35	240	Yes
R-AlN	1.6-1.1	25	250	No

The GaN and AlN growth rates homogeneity can be evaluated by measuring the thickness of GaN and AlN layers using SEM cross-section images (see supplementary materials). The GaN and AlN thicknesses are respectively 11% and 30% thinner at the edges (20 mm away from the center). In particular, this induces a decrease of the nanomask thickness at the edges and a variation in the

porosity. By studying the samples as a function of the position, this grants access to a large number of porosities. The data shown will be identified by the label x/t for each sample, where x is the AlN mask thickness in mono-layers (MLs) and t the sublimation time in min.

b. Scanning electron microscopy observations

The samples were observed using scanning electron microscopy in plan-view (Figure 1a-h) and cross-section (Figure 2a-c). The porosity is evaluated from plan-view images by dividing the pore surface area by the total surface area. As shown in Figure 1, the porosity can be varied in a very large range from 0.04 to 0.9. For small porosities (<0.3), the pores are almost isolated (Figure 1a-d), while for larger porosities, the pores coalesce. As expected, the porosity increases when the AlN nanomask thickness decreases. For sample 4.7/25, the mean equivalent pore diameter[1] is 49 nm and the pore density is $2.0x10^9$ cm^{-2}. For sample 3.3/25, the mean equivalent pore diameter is 71 nm and the pore density is $5.4x10^9$ cm^{-2}. The increase of the pore density and diameter appears directly connected with the decrease of the AlN nanomask thickness (when the sublimation conditions are identical). The AlN nanomask thickness is 2.5 MLs for both samples 2.5/20 and 2.5/30, whereas the sublimation time is 20 min. and 30 min., respectively. The porosity / mean equivalent diameter / pore density are 0.32 / 54.1 nm / $1.4x10^{10}$ cm^{-2} and 0.44 / 104.6 nm / $5.2x10^9$ cm^{-2} for the samples 2.5/20 and 2.5/30, respectively. This shows that, for a given AlN nanomask size, when the sublimation time increases, the lateral pore size increases and the pore density decreases due to their coalescence. Therefore, it is important to consider both the sublimation time and the AlN nanomask thickness to control the porosity and the pore distribution.

For a small AlN nanomask thickness of 0.8 ML and a sublimation time of 35 min. (sample 0.8/35), Figure 1h), most of the GaN has been sublimated and we cannot *stricto sensu* describe the sample as porous. In this case, it would be more appropriate to replace the term porosity by 1-c, where c is the GaN coverage of the surface. In the following, the term porosity will be used by simplicity even for low GaN coverages. For sample 0.8/35, as shown in Figure 1h, only narrow GaN nanowires are remaining on the surface. The diameter of isolated nanowires can be smaller than 10 nm. This has a strong influence on the PL peak energy as it will be discussed later.

[1] The equivalent pore diameter corresponds to the diameter of a circle whose surface equals the pore surface extracted from the top-view SEM images.

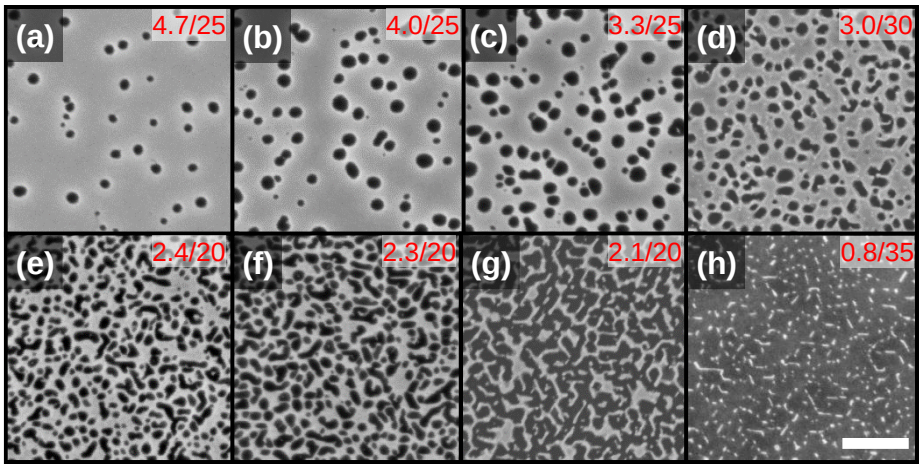

Figure 1. Top view scanning microscope images of selected porous GaN samples made by sublimation through an AlN nanomask. The numbers in each upper right corner correspond to the AlN nanomask thickness in mono-layers / sublimation time in min. The porosity evaluated from these images is (a) 0.04, (b) 0.1, (c) 0.2, (d) 0.3, (e) 0.43, (f) 0,5, (g) 0.63, (h) 0.9. The scale bar is 400 nm.

From SEM cross-section images (Figure 2a, b, c), we can see that the pores have vertical sidewalls. This specific morphology comes from the anisotropic nature of the wurtzite structure and the difference in the surface energies of GaN planes parallel or perpendicular to the surface. The surface energy of the (0001) plane is smaller than the one of (1-100) and (11-20) planes.[23] Therefore, the sublimation rate of the (0001) plane is expected to be larger. Experimentally, we effectively found that the vertical over horizontal sublimation rate ratio under vacuum was about 1%.[24] Note that, in principle, as pointed out in Refs. [25] and [26]**,** the crystal shape should be defined by the planes dissolving the fastest. This is not the case here because there is mask on the top surface which locally blocks the sublimation along the (0001) plane.

For the samples shown in Figure 2, the pores are reaching the AlN surface. Their depth is at its maximum value corresponding to the initial GaN thickness. It is not the case for sample 2.5/20 (Table 1), for which the sublimation time was not long enough to fully sublimate the GaN down to the AlN buffer layer. From the observed mean pore depth for this sample, we can deduce a sublimation rate of ~10 nm/min. This rate is much slower than the one reported in Ref. [27] for GaN evaporated under vacuum, which was close to 100 nm / min (by extrapolating the value at 900°C). This can be explained by the fact that a small NH_3 flow reduces the sublimation rate, leading to a competition between reabsorption and sublimation inside the forming pores.

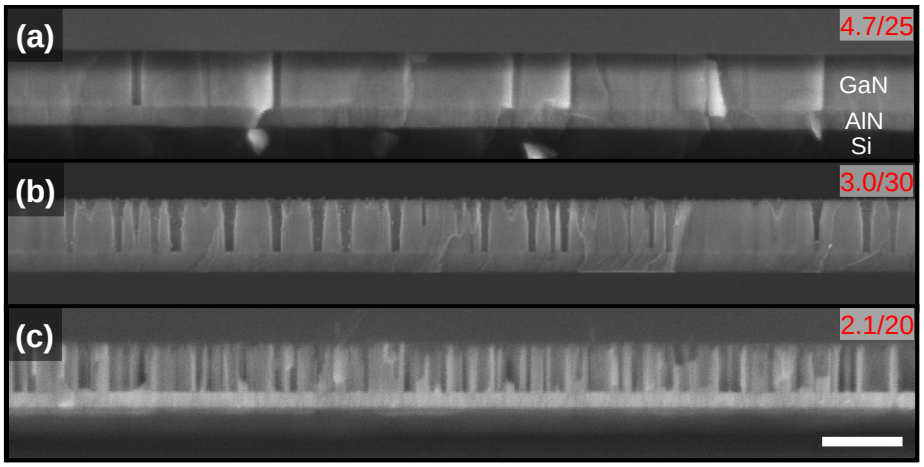

Figure 2. Cross section scanning microscope images of porous GaN made by sublimation through an AlN nanomask. The numbers in each upper right corner correspond to the AlN nanomask thickness in mono-layers / sublimation time in min. The corresponding porosity extracted from top-view scanning electron microscopy images is (a) 0,04, (b) 0,3, (c) 0,63. The scale bar is 400 nm.

It is important to stress out that the AlN mask thickness exceeds 1 mono-layer for most of these samples. For such coverage, the AlN completely covers the surface. Therefore, the simple picture of a mask formed with apertures inside does not apply in this case. Actually, the sublimation probably starts at places where dislocations emerge at the surface. These defects constitute "weak" points where the sublimation can be initiated. Grain boundaries, with dislocations grouped in a limited surface area, could thus constitute preferential sublimation sites. One observation supporting this hypothesis is that when the dislocation density decreases, the AlN mask thickness requested to make the GaN porous has to be decreased as it will be shown in section 4.

c. Photoluminescence properties

The PL properties of these samples were measured at room temperature with the 244 nm line of a frequency doubled Ar laser at an output power of 27 mW as the excitation source. Figure 3a shows some examples of these spectra for samples with different porosities. The PL peak intensities (Figure 3b) and the PL peak energy (Figure 3c) are extracted from the PL spectra of all the samples. NP1 sample has the lowest PL intensity. NP2 and NP3 samples have a PL intensity almost 10 times larger than NP1. The difference is the thin AlN layer (2.5 ML) on top of the structures of samples NP2 and NP3. This layer can constitute a barrier for excitons in the GaN layer and block their diffusion towards the surface where the excitons can recombine non-radiatively.[28][29] NP2 and NP3 have very similar PL intensities which indicate that the temperature ramp used for sample NP3 has no impact on the PL properties. For porous GaN samples, the PL intensity increases with the porosity up to a porosity of ~0.6 and then decrease for larger porosities. The maximum PL intensity of the porous GaN with AlN nanomask is 168 times larger than the sample NP2. The large enhancement of the room temperature

PL intensity of porous GaN made by sublimation with a Si_xN_y nanomask was previously attributed to several factors such as the preferential sublimation of dislocation cores, the depolarization effect, and to an enhanced extraction efficiency. [18] [19] [20] The PL peak intensity was also corrected by the material volume (by dividing the intensity by a factor 1-porosity). This does not change the general aspect of the curve giving the PL peak intensity as a function of the porosity (not shown). The PL intensity of sample P4 is much smaller than that of the other porous samples. This can be explained by the morphology of the layer. The remaining GaN forms nanowires with diameters as small as 10 nm. This could increase surface non-radiative recombination and decrease the light coupling of the laser inside the nanowires.

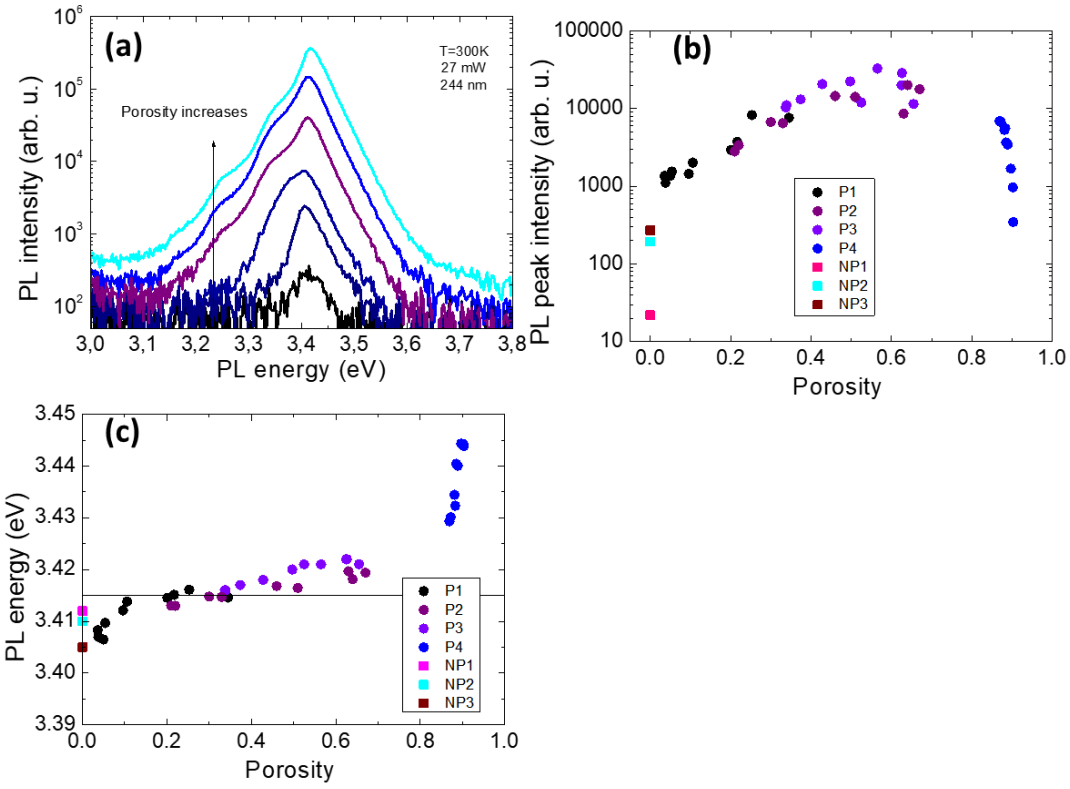

Figure 3. Room temperature photoluminescence properties of non-porous and porous GaN with an AlN nanomask. (a) Examples of photoluminescence spectra. From the lowest to the highest intensity, the spectra were measured on samples NP1, NP2, 4.7/25, 3.1/30, 2.5/20, and 2.1/20. The corresponding porosities are 0, 0, 0.04, 0.2, 0.32, and 0.63. (b) Photoluminescence peak intensity as a function of the porosity. (c) Photoluminescence peak energy of the GaN band-edge as a function of the porosity.

The PL peak energy of the GaN band-edge can give us information about the strain state of the GaN layer.[30] For a strain-free GaN layer, the room temperature PL peak energy of the A exciton is 3.415 eV.[31] For the non-porous samples NP1, NP2 and NP3, the PL peak energy is between 3.405 eV and 3.412 eV. This corresponds to a slight tensile strain. This strain is related to the mismatch of the thermal

expansion coefficients between the silicon substrate and the nitride layers, the in-plane lattice parameter shrinking of silicon during the cooling-down after growth being larger.[32] For very small porosities below 0.1, the strain state of porous GaN layers is very similar to that of non-porous GaN. For larger porosities up to 0.7, the PL peak position indicates nearly strain-free layers with a tendency to obtain a slight compressive stress for porosities of 0.6-0.7. A strong change is observed for the samples with the largest porosity (above 0.9) for which a strong shift towards high energies up to 3.445 eV is observed. Such an abrupt shift was previously observed for narrow GaN nanowires and attributed to dielectric confinement.[33] The small diameter nanowires (below 10 nm) obtained for sample P4 is compatible with this interpretation. Also, a contribution of surface stress can further explain this large PL shift.[34]

3. Comparison with porous GaN made using sublimation through a Si_xN_y nanomask

The objective of this section is to compare the properties of porous GaN made by selective area sublimation, eitherwith a self-organized AlN nanomask or with a Si_xN_y nanomask used in previous works.[17] [18] [19] [20] [21] The structure of the samples with a Si_xN_y nanomask is very similar to the one studied above. It consists in a GaN (250 nm) / AlN (100 nm) stack grown on a Si(111) substrate by MBE.[17] The pores have very different sizes and densities depending on the nanomask nature. This is especially clear for small porosities (Figure 4a and b) for which the pores are almost not coalesced. Figure 4a and b show porous GaN samples both with a porosity of 0.11. The pore density / mean diameter is $1.0x10^{11}$ cm^{-2} / 11.8 nm and $3.3x10^{9}$ cm^{-2} / 64.4 nm for the samples with the Si_xN_y and AlN nanomask, respectively. As it was previously studied by transmission electron microscopy, in the case of a Si_xN_y nanomask, there is a preferential sublimation of the dislocation cores [20] and therefore the pore density is at least equal to the dislocation density. The situation is quite different for the AlN nanomask for which the pore density is much smaller. This indicates that all the dislocation cores are not sublimated and this is probably due to the larger thickness of the AlN nanomask (i.e. above 3ML) for the sample shown in Figure 4b. If larger Si_xN_y nanomask thicknesses are used (~ 2 MLs), the sublimation is completely stopped and the formation of pores is not observed. This means that the Si_xN_y nanomask is more stable than the AlN nanomask and that in the vicinity of defective areas, the AlN nanomask can decompose more rapidly. In the case of thick layers, the sublimation rate of GaN is much larger than AlN.[27][35][36] For example, to achieve a sublimation rate of 1 nm/s, the temperature has to be 890°C for GaN and 1420°C for AlN. In principle, according to our sublimation conditions the sublimation of AlN should be completely negligible. Therefore, we infer that the

sublimation of AlN is probably induced by the sublimation of the GaN below the nanomask which weakens the thin AlN layer on top.

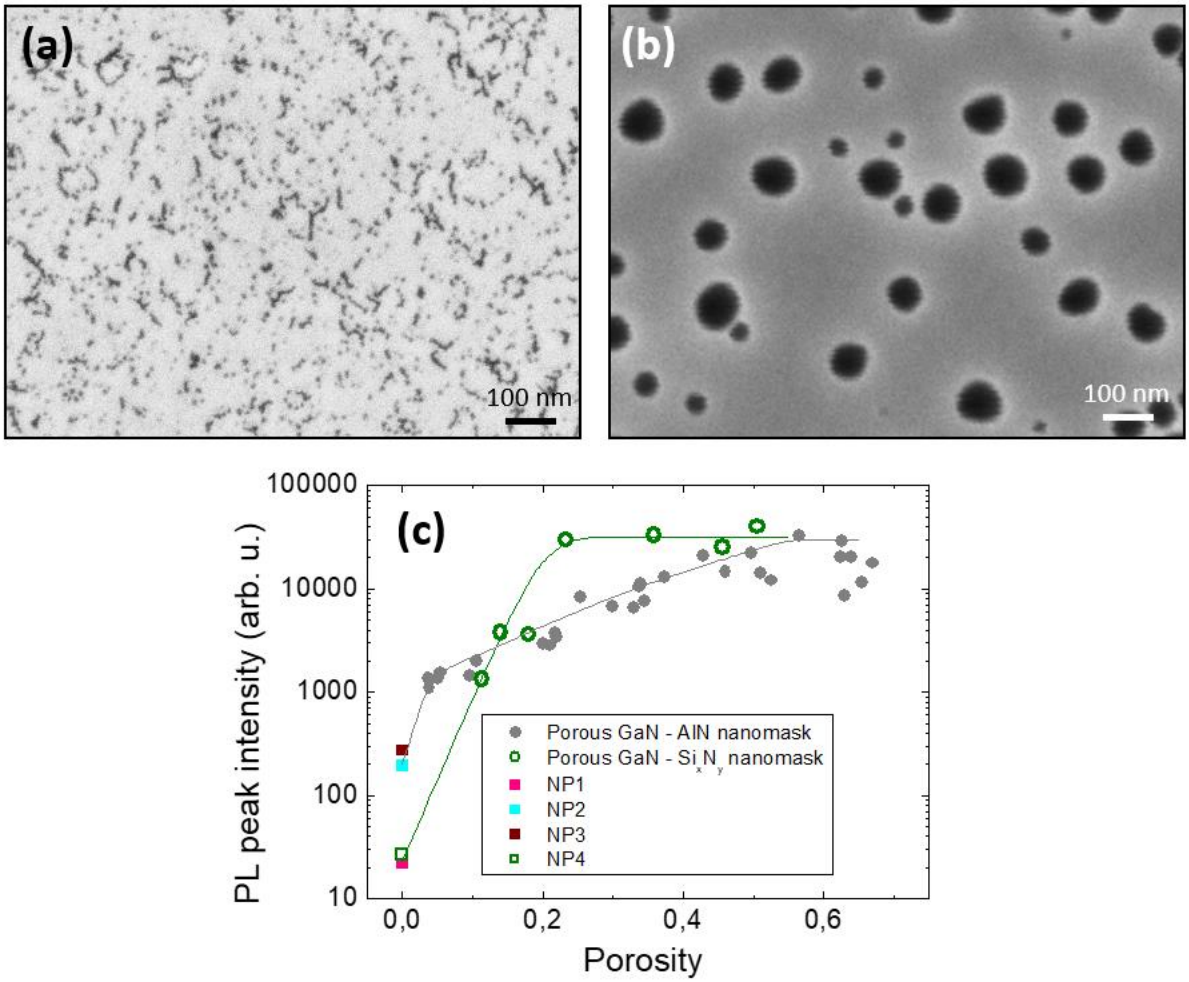

Figure 4. Top view scanning electron microscopy images of porous GaN samples with a porosity of 0.11 made by sublimation through a Si_xN_y (a) or an AlN nanomask corresponding to sample 4/25 (b). (c) Photoluminescence peak intensity at room temperature of the GaN band-edge as a function of the porosity for porous GaN made by sublimation with a Si_xN_y or an AlN nanomask. The lines are guides for the eye. The photoluminescence intensities of all the samples can be compared using the PL peak intensity values since they all have been calibrated with a reference sample.

Figure 4c shows the variation of the PL peak intensity of the GaN band-edge as a function of the porosity of sublimated porous GaN made either by using a Si_xN_y or an AlN nanomask. A strong increase of the PL intensity is observed for both series of samples when the porosity increases (up to 0.65). The main difference is that the slope of the PL rise is larger for the samples with a Si_xN_y nanomask. The maximum intensity is almost reached for a porosity of 0.25 for the samples with Si_xN_y nanomask while it has to be 0.55 for the samples with an AlN nanomask. This indicates that to get the maximum PL intensity, all the dislocation cores have to be sublimated and this can be obtained either for GaN layers with a high density of small pores or for GaN layers with a large porosity. In the perspective of keeping

the largest material volume with the highest PL intensity, the use of a Si_xN_y nanomask appears as a better choice than the AlN nanomask.

4. Regrowth on porous GaN

a. Fabrication of the samples

The initial samples used for this study are light emitting diode structures grown by metal-organic vapor phase epitaxy (MOVPE) on Si(111) substrates in a 7x2 in. showerhead reactor. The buffer layers (starting from the substrate) are constituted by the following layer stack: AlN (230 nm), GaN (2200 nm), AlN (20 nm), GaN (800 nm), AlN (20 nm) and GaN (500 nm). On top of this template is grown an LED structure composed by n-GaN (1 µm), an n-InGaN/GaN short period superlattice (46 nm), an undoped InGaN/GaN multiple quantum well (84 nm) and p-GaN layers (120 nm). The threading dislocation density emerging at the surface is estimated to 1-2x10^9 cm^{-2} on these samples.

Such 2 in. LED structures from the same MOVPE run were made porous using either a Si_xN_y (sample R-SiN) or an AlN nanomask (sample R-AlN). This step was realized in a MBE system with two chambers connected under ultra-high vacuum. In one chamber, the samples were made porous and then in the other chamber a 100 nm thick p-GaN was grown at 770°C on each sample. For the sample R-SiN, the surface was exposed to the flux of a Si cell heated at 1250°C for 13 min. Then, the sample was heated at 900°C for the selective area sublimation with an ammonia flow of 10 sccm for 60 min. and under vaccum for 13 min. For the sample R-AlN, a 1.6 ML thick AlN layer was grown on top of the structure. The sublimation was performed at 900°C under an effective ammonia flow of 2 sccm (pulsed conditions) for 20 min. Note that the AlN nanomask thickness has to be reduced in order to get a porous layer compared to the samples studied in the first section. For example, for a sample with a similar crystalline quality and an AlN nanomask thickness of 2.8 MLs, a sublimation time of 25 min. at 900°C with an effective ammonia flow of 2 sccm, the formation of pores is not observed, while for such conditions the porosity is larger than 0.4 for the samples discussed above. This illustrates the importance of the defect density in the selective area sublimation process and the formation of pores.

b. SEM observations

The MBE p-GaN regrowth is very different depending on the nature of the nanomask. In the case of a Si_xN_y nanomask (Figure 5a and c), the GaN grows inside the pores down to a depth of ~50 nm and also above the mask to form a shape similar to an ice cream on a stick. Figure 5a shows that there is a significant lateral growth. In the case of an AlN nanomask (Figure 5b and d), the GaN nucleates directly on the AlN layer and grows exclusively vertically. The consequence is that the pore diameter does not evolve during the overgrowth. For both samples, we observe the formation of inclined facets with an

angle of 62° relative to the (0001) plane corresponding to {10-11} planes. Schematics of the obtained morphologies are shown in Figure 5e and f. The morphology obtained for R-AlN is quite obvious to understand while it is more complex for sample R-SiN. For this last sample, our interpretation is that the GaN first nucleates on the sidewalls of the pores below the Si_xN_y nanomask. Then, from these sites, the GaN can grow vertically and encapsulate the Si_xN_y. In the end, this process leads to almost coalesced GaN layers.

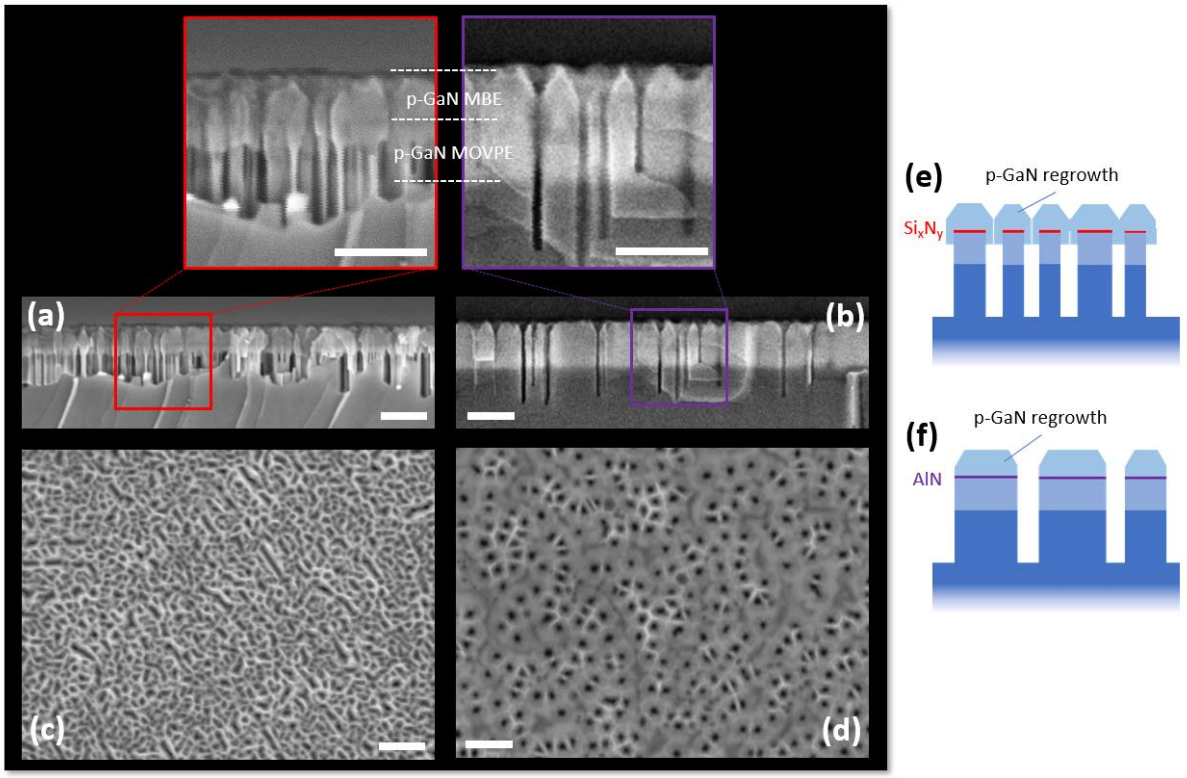

Figure 5. Scanning electron microscopy images in cross-section (a)(b) and in plan-view (c)(d) of porous light emitting diodes structures overgrown by a nominally 100 nm p-GaN layer by molecular beam epitaxy. The structures were made porous using selective area sublimation through a Si_xN_y nanomask (a)(c) and an AlN nanomask (b)(d). The scale bars correspond to 100 nm. (e)(f) Schematics illustrating the p-GaN regrowth on the porous layers by molecular beam epitaxy.

5. Conclusion

We have shown that porous GaN can be obtained by selective area sublimation with different nanomasks such as Si_xN_y and AlN. We anticipate that more generally other materials can be used for such a goal provided that the mask material can withstand high enough temperatures for the sublimation of GaN. Depending on the choice of the self-organized nanomask, pores with very different morphologies can be obtained: their density can be varied over more than an order of magnitude and their diameter can be changed by a factor of ~6. The GaN pores are larger and denser when the AlN nanomask thickness decreases and the sublimation time increases. The formation of pores in GaN

using an AlN nanomask is highly dependent on the dislocation density: for a same AlN nanomask thickness, the annealed GaN layer can become porous or keep a 2-dimensional morphology. We found that the AlN nanomask can be sublimated around pores, this process being driven by the underneath GaN sublimation. The room temperature photoluminescence intensity of thin porous GaN/AlN layers on Si(111) substrate can be improved by several orders of magnitude whatever the nanomask used. The maximum PL intensity is obtained at a lower porosity with a Si_xN_y nanomask compared to an AlN nanomask as a result of a higher pore density, which is favorable to suppress the dislocation cores. The regrowth of GaN by molecular beam epitaxy on porous layers is highly dependent on the nanomask. Almost fully coalesced GaN layers are obtained on porous GaN with a Si_xN_y nanomask, while the pore diameter stays almost unchanged after regrowth on porous GaN with an AlN nanomask.

Acknowledgments

This work has been supported by the French National Research Agency (ANR) through the project NAPOLI (ANR-18-CE24-0022).

Data availability statement

All data that support the findings of this study are included within the article (and any supplementary files).

References

1. L. T. Canham, "Silicon quantum wire array fabrication by electrochemical and chemical dissolution of wafers," Appl. Phys. Lett. **57**(10), 1046–1048 (1990).
2. G. Gesele, J. Linsmeier, V. Drach, J. Fricke, and R. Arens-Fischer, "Temperature-dependent thermal conductivity of porous silicon," J. Phys. Appl. Phys. **30**(21), 2911–2916 (1997).
3. Y. Watanabe, Y. Arita, T. Yokoyama, and Y. Igarashi, "Formation and Properties of Porous Silicon and Its Application," J. Electrochem. Soc. **122**(10), 1351–1355 (1975).
4. S. I. Romanov, V. I. Mashanov, L. V. Sokolov, A. Gutakovskii, and O. P. Pchelyakov, "GeSi films with reduced dislocation density grown by molecular-beam epitaxy on compliant substrates based on porous silicon," Appl. Phys. Lett. **75**(26), 4118–4120 (1999).
5. S. S. Pasayat, C. Gupta, D. Acker-James, D. A. Cohen, S. P. DenBaars, S. Nakamura, S. Keller, U. K. Mishra, and Fellow, IEEE, "Fabrication of relaxed InGaN pseudo-substrates composed of micron-sized pattern arrays with high fill factors using porous GaN," Semicond. Sci. Technol. **34**(11), 115020 (2019).
6. V. S.-Y. Lin, K. Motesharei, K.-P. S. Dancil, M. J. Sailor, and M. R. Ghadiri, "A Porous Silicon-Based Optical Interferometric Biosensor," Science **278**(5339), 840–843 (1997).
7. O. V. Bilousov, J. J. Carvajal, H. Geaney, V. Z. Zubialevich, P. J. Parbrook, O. Martínez, J. Jiménez, F. Díaz, M. Aguiló, and C. O'Dwyer, "Fully Porous GaN p–n Junction Diodes Fabricated by Chemical Vapor Deposition," ACS Appl. Mater. Interfaces **6**(20), 17954–17964 (2014).
8. C. Zhang, S. H. Park, D. Chen, D.-W. Lin, W. Xiong, H.-C. Kuo, C.-F. Lin, H. Cao, and J. Han, "Mesoporous GaN for Photonic Engineering—Highly Reflective GaN Mirrors as an Example," ACS Photonics **2**(7), 980–986 (2015).
9. L. Zhang, S. Wang, Y. Shao, Y. Wu, C. Sun, Q. Huo, B. Zhang, H. Hu, and X. Hao, "One-step fabrication of porous GaN crystal membrane and its application in energy storage," Sci. Rep. **7**, 44063 (2017).
10. L. Liu, C. Yang, A. Patanè, Z. Yu, F. Yan, K. Wang, H. Lu, J. Li, and L. Zhao, "High-detectivity ultraviolet photodetectors based on laterally mesoporous GaN," Nanoscale (2017).
11. K. J. Lee, S. Oh, S.-J. Kim, S.-Y. Yim, N. Myoung, K. Lee, J. S. Kim, S. H. Jung, T.-H. Chung, and S.-J. Park, "Enhanced optical output in InGaN/GaN light-emitting diodes by tailored refractive index of nanoporous GaN," Nanotechnology **30**(41), 415301 (2019).
12. J. C. Jarman, T. Zhu, P. H. Griffin, and R. A. Oliver, "Light-output enhancement of InGaN light emitting diodes regrown on nanoporous distributed Bragg reflector substrates," Jpn. J. Appl. Phys. **58**(SC), SCCC14 (2019).
13. S. M. Mishkat-Ul-Masabih, A. A. Aragon, M. Monavarian, T. S. Luk, and D. F. Feezell, "Electrically injected nonpolar GaN-based VCSELs with lattice-matched nanoporous distributed Bragg reflector mirrors," Appl. Phys. Express **12**(3), 036504 (2019).
14. S. S. Pasayat, R. Ley, C. Gupta, M. S. Wong, C. Lynsky, Y. Wang, M. J. Gordon, S. Nakamura, S. P. Denbaars, S. Keller, and U. K. Mishra, "Color-tunable **<** 10 μ m square InGaN micro-LEDs on compliant GaN-on-porous-GaN pseudo-substrates," Appl. Phys. Lett. **117**(6), 061105 (2020).
15. P. H. Griffin and R. A. Oliver, "Porous nitride semiconductors reviewed," J. Phys. Appl. Phys. **53**(38), 383002 (2020).
16. P. Pandey, M. Sui, M.-Y. Li, Q. Zhang, S. Kunwar, J. Wu, Z. M. Wang, G. J. Salamo, and J. Lee, "Nanoparticles to Nanoholes: Fabrication of Porous GaN with Precisely Controlled Dimension via the Enhanced GaN Decomposition by Au Nanoparticles," Cryst. Growth Des. **16**(6), 3334–3344 (2016).
17. B. Damilano, S. Vézian, and J. Massies, "Mesoporous GaN Made by Selective Area Sublimation for Efficient Light Emission on Si Substrate," Phys. Status Solidi B 1700392 (2017).
18. B. Damilano, S. Vézian, and J. Massies, "Photoluminescence properties of porous GaN and (Ga,In)N/GaN single quantum well made by selective area sublimation," Opt. Express **25**(26), 33243 (2017).

19. T. H. Ngo, B. Gil, T. V. Shubina, B. Damilano, S. Vezian, P. Valvin, and J. Massies, "Enhanced excitonic emission efficiency in porous GaN," Sci. Rep. **8**(1), 15767 (2018).
20. B. Damilano, S. Vézian, M. P. Chauvat, P. Ruterana, N. Amador-Mendez, S. Collin, M. Tchernycheva, P. Valvin, and B. Gil, "Preferential sublimation along threading dislocations in InGaN/GaN single quantum well for improved photoluminescence," J. Appl. Phys. **132**(3), 035302 (2022).
21. N. Amador-Mendez, T. Mathieu-Pennober, S. Vézian, M.-P. Chauvat, M. Morales, P. Ruterana, A. Babichev, F. Bayle, F. H. Julien, S. Bouchoule, S. Collin, B. Gil, N. Tappy, A. Fontcuberta i Morral, B. Damilano, and M. Tchernycheva, "Porous Nitride Light-Emitting Diodes," ACS Photonics **9**(4), 1256–1263 (2022).
22. T. Markurt, L. Lymperakis, J. Neugebauer, P. Drechsel, P. Stauss, T. Schulz, T. Remmele, V. Grillo, E. Rotunno, and M. Albrecht, "Blocking Growth by an Electrically Active Subsurface Layer: The Effect of Si as an Antisurfactant in the Growth of GaN," Phys. Rev. Lett. **110**(3), (2013).
23. C. E. Dreyer, A. Janotti, and C. G. Van de Walle, "Absolute surface energies of polar and nonpolar planes of GaN," Phys. Rev. B **89**(8), 081305 (2014).
24. S. Sergent, B. Damilano, S. Vézian, S. Chenot, M. Takiguchi, T. Tsuchizawa, H. Taniyama, and M. Notomi, "Subliming GaN into Ordered Nanowire Arrays for Ultraviolet and Visible Nanophotonics," ACS Photonics **6**(12), 3321–3330 (2019).
25. R. C. Snyder and M. F. Doherty, "Faceted crystal shape evolution during dissolution or growth," AIChE J. **53**(5), 1337–1348 (2007).
26. T. Auzelle, G. Calabrese, and S. Fernández-Garrido, "Tuning the orientation of the top-facets of GaN nanowires in molecular beam epitaxy by thermal decomposition," Phys. Rev. Mater. **3**(1), (2019).
27. N. Grandjean, J. Massies, F. Semond, S. Y. Karpov, and R. A. Talalaev, "GaN evaporation in molecular-beam epitaxy environment," Appl. Phys. Lett. **74**(13), 1854–1856 (1999).
28. P. Šcˇajev, K. Jarašiūnas, S. Okur, Ü. Özgür, and H. Morkoç, "Carrier dynamics in bulk GaN," J. Appl. Phys. **111**(2), 023702 (2012).
29. G. L. Martinez, M. R. Curiel, B. J. Skromme, and R. J. Molnar, "Surface recombination and sulfide passivation of GaN," J. Electron. Mater. **29**(3), 325–331 (2000).
30. B. Gil, O. Briot, and R.-L. Aulombard, "Valence-band physics and the optical properties of GaN epilayers grown onto sapphire with wurtzite symmetry," Phys. Rev. B **52**(24), R17028–R17031 (1995).
31. B. Monemar, P. P. Paskov, J. P. Bergman, A. A. Toropov, T. V. Shubina, T. Malinauskas, and A. Usui, "Recombination of free and bound excitons in GaN," Phys. Status Solidi B **245**(9), 1723–1740 (2008).
32. A. Krost, A. Dadgar, G. Strassburger, and R. Clos, "GaN-based epitaxy on silicon: stress measurements," Phys. Status Solidi A **200**(1), 26–35 (2003).
33. J. K. Zettler, P. Corfdir, C. Hauswald, E. Luna, U. Jahn, T. Flissikowski, E. Schmidt, C. Ronning, A. Trampert, L. Geelhaar, H. T. Grahn, O. Brandt, and S. Fernández-Garrido, "Observation of Dielectrically Confined Excitons in Ultrathin GaN Nanowires up to Room Temperature," Nano Lett. **16**(2), 973–980 (2016).
34. G. Calabrese, D. van Treeck, V. M. Kaganer, O. Konovalov, P. Corfdir, C. Sinito, L. Geelhaar, O. Brandt, and S. Fernández-Garrido, "Radius-dependent homogeneous strain in uncoalesced GaN nanowires," Acta Mater. **195**, 87–97 (2020).
35. Z. . Fan and N. Newman, "Experimental determination of the rates of decomposition and cation desorption from AlN surfaces," Mater. Sci. Eng. B **87**(3), 244–248 (2001).
36. Y. Kumagai, K. Akiyama, R. Togashi, H. Murakami, M. Takeuchi, T. Kinoshita, K. Takada, Y. Aoyagi, and A. Koukitu, "Polarity dependence of AlN {0 0 0 1} decomposition in flowing H2," J. Cryst. Growth **305**(2), 366–371 (2007).